Electronic Supplementary Material (ESI) for Physical Chemistry Chemical Physics.

Supporting Information

Effect of Defect Types on the Electronic and Optical Properties of Graphene Nanoflakes Physisorbed by Ionic liquids

Mehdi Shakourian-Fard[†*], Ganesh Kamath[‡]

[†]Birjand University of Technology, Department of Chemical Engineering, Birjand, P.O. Box 97175/569, Iran.

[‡]Department of Chemistry, University of Missouri-Columbia, Columbia, MO 65211, USA

*Corresponding author: shakourian@birjandut.ac.ir; m_shakori1361@yahoo.com

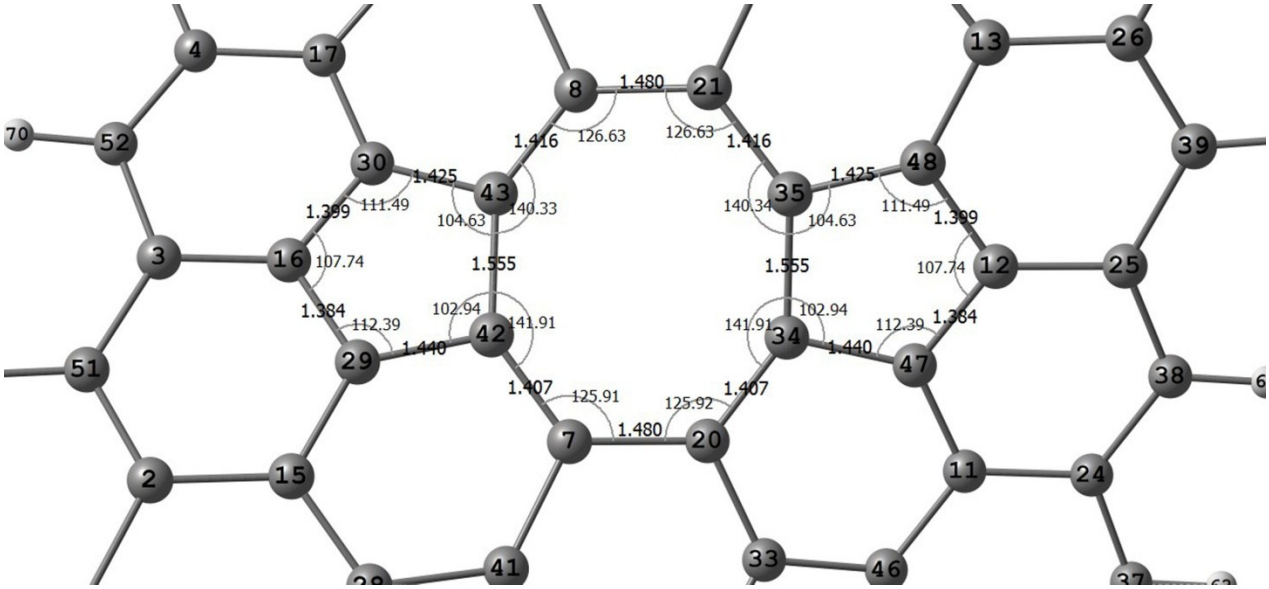

a) DV(5-8-5) DG surface

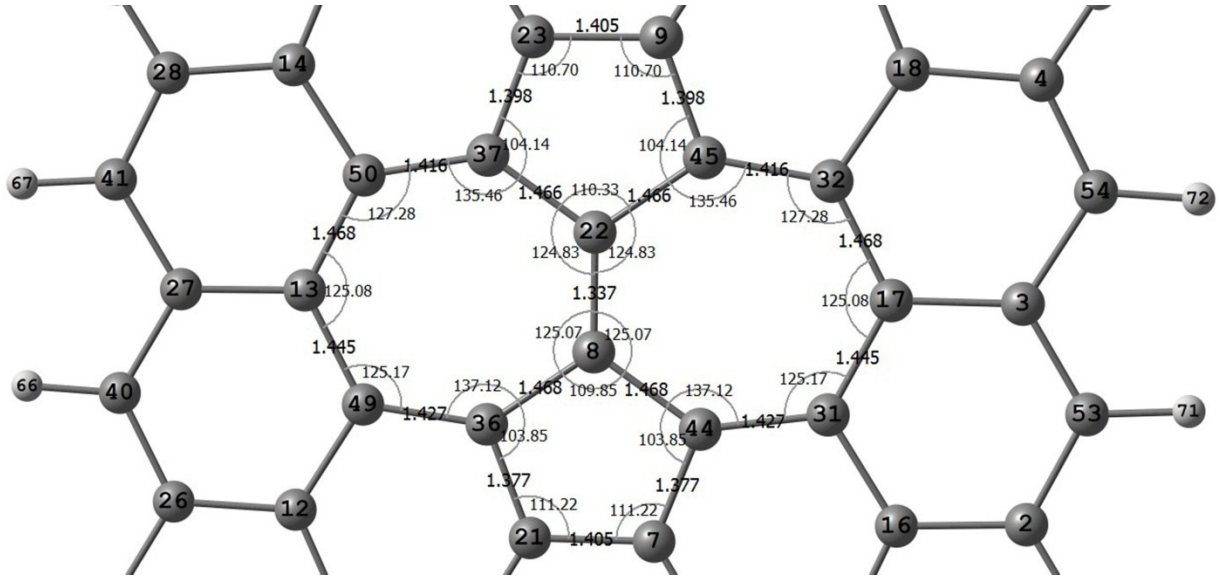

b) SW(55-77) DG surface

Fig S1. The bond lengths (in Å) and bond angles (in degrees) in the optimized structures of a) DV(5-8-5)-GNF surface and b) SW(55-77)-GNF surface at the M06-2X/cc-pVDZ level of theory.

Bond lengths and bond angles at the 5-8-5 and 55-77 defect parts of the DV-GNF and SW-GNF models were calculated and also shown in Fig. S1. Comparing with literature,[1] the calculated C-C bond lengths at the defect parts are different from those at the GNF model presented for pristine graphene. As seen from Fig S1a, the pentagonal rings in the DV-GNF model have pair-wise equal bond lengths and bond angles. On the other hand, the bond lengths and bond angles in the octagonal ring are pairwise symmetrical. The C42-C43 and C34-C35 bonds in the DV-GNF model which are common bonds between the pentagonal and octagonal rings are equal and have the largest bond lengths about 1.555 Å. In the case of SW-GNF model, the C8-C22 bond which is regarded as a common bond between the heptagonal rings has the shortest bond length about 1.337 Å. In addition, the common bond pairs between pentagonal and heptagonal rings (C22-C37, C22-C45 and C8-C36, C8-C44) have bond lengths about 1.466 Å and 1.468 Å, respectively. On the other hand, the bond lengths and bond angles in the pentagonal rings and heptagonal rings are pair-wise symmetrical.

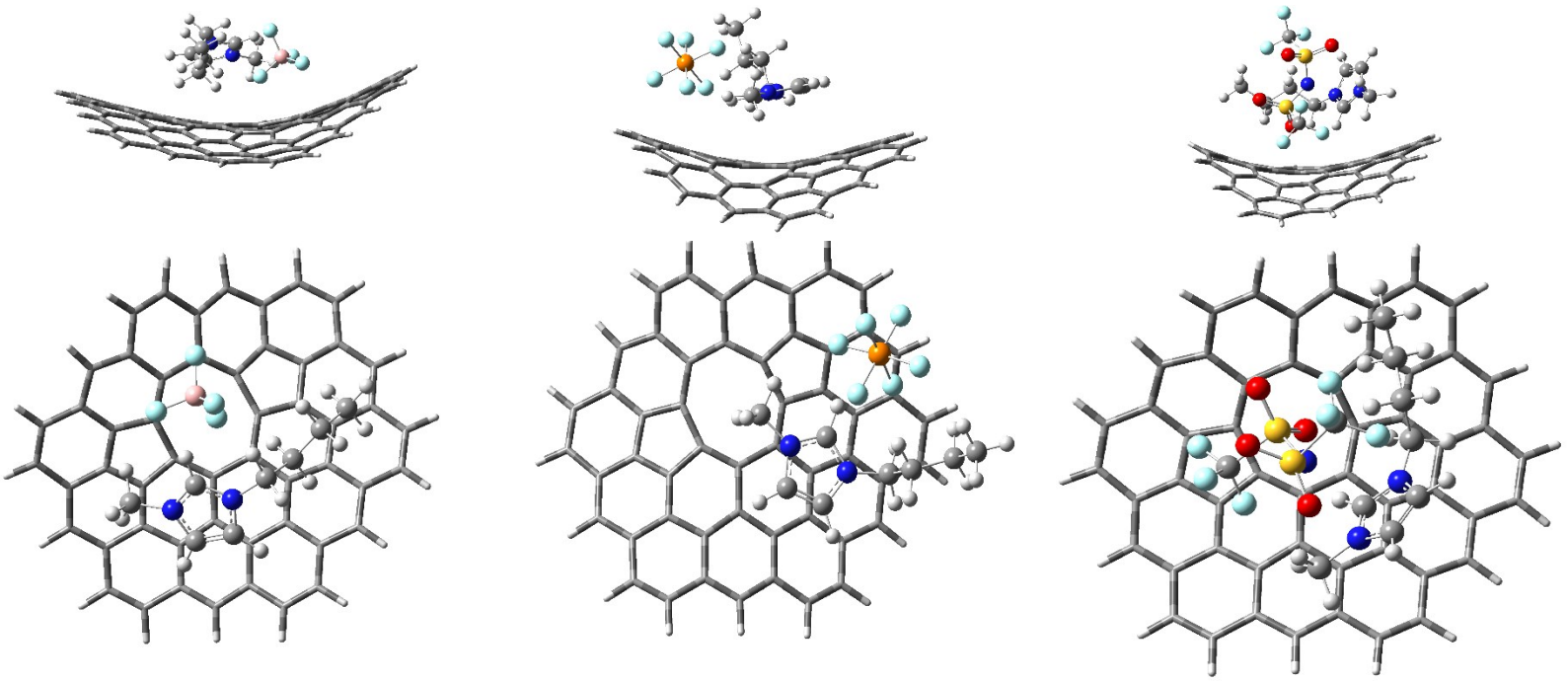

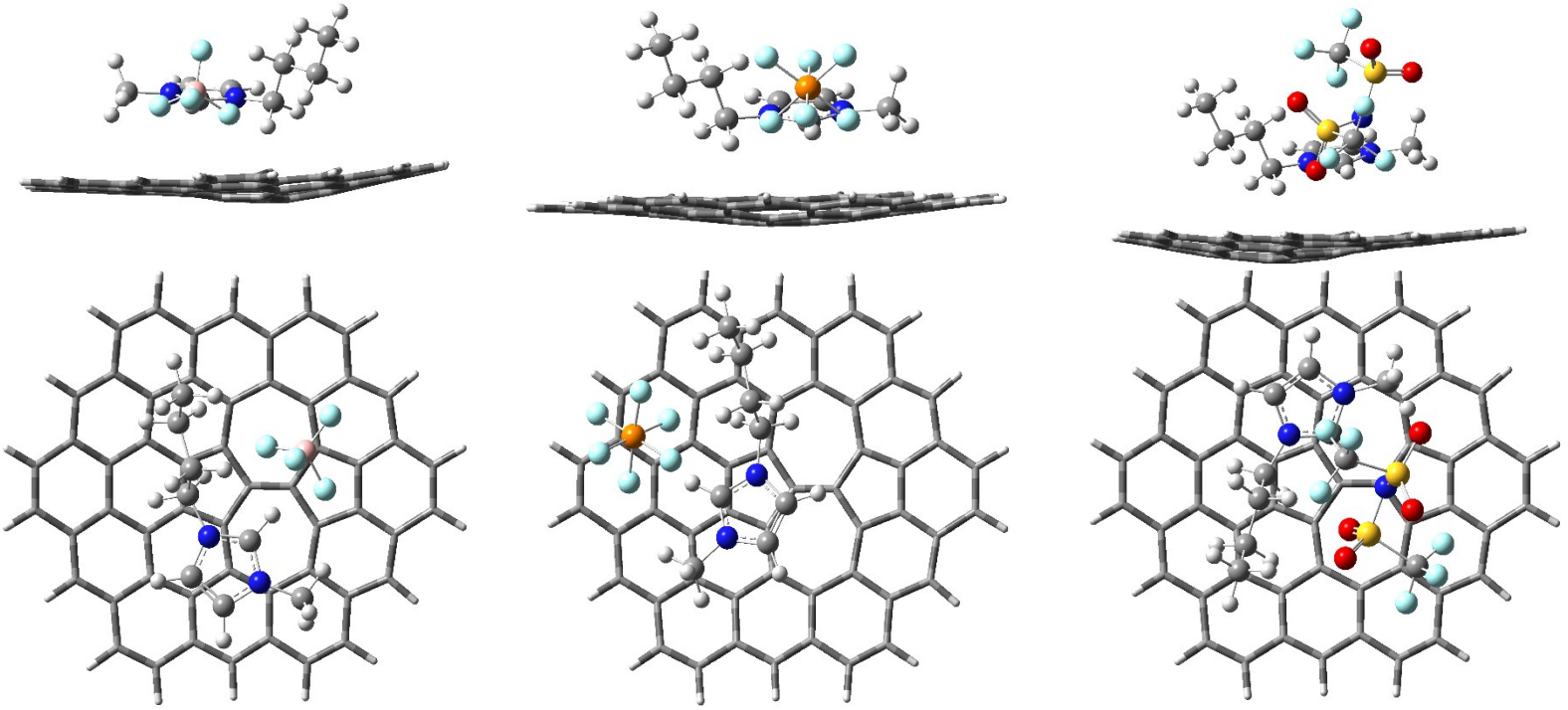

Fig S2. The most stable geometries of DV(SW)-GNF…IL (IL = [Bmim][Y] (Y = BF_4^-, PF_6^-, and Tf_2N^-)) complexes.

1. Ionic Liquids

In order to find the most stable geometries of ILs considered in this study, we applied the method described in our previous works.[2-3] In this method, the region around the most stable geometry of $[Bmim]^+$ cation is divided into several regions and then the most stable geometry of anion is located in these regions. There are also some sub-configurations in each region which are related to different orientations of anion with respect to the cation. For example, $[BF_4]^-$ anion could interact with the cation through one, two, and three of its fluorine atoms in each region. Finally, all designed structures for interaction of $[Bmim]^+$ cation with $[BF_4]^-$, $[PF_6]^-$, and $[Tf_2N]^-$ anions were fully optimized at the M06-2X/cc-pVDZ level of theory. The position of the anion relative to $[Bmim]^+$ cation in the most stable geometries of ILs is seen in Fig 1. Our calculations indicate that the anions tend to interact with $[Bmim]^+$ cation through C-H bond of imidazolium ring and C-H bonds of methyl and butyl groups. Our previous calculations[2-3] at the M06-2X/cc-pVDZ level of theory have also indicated that the interaction of $[BF_4]^-$, $[PF_6]^-$, and $[Tf_2N]^-$ anions with $[Bmim]^+$ cation is hydrogen bond type and is classified as a closed-shell (electrostatic) interaction in the nature. In addition, the stability of ILs was evaluated by binding energy (ΔE_b) values corrected by basis set superposition errors (BSSEs). The order of binding energies for these ILs is found to be $[Bmim][BF_4]$ (-87.66 kcal/mol)> $[Bmim][PF_6]$ (-81.05 kcal/mol)> $[Bmim][Tf_2N]$ (-80.15 kcal/mol). It is evident that there is a considerable decrease in the ΔE_b values with increasing size of anion from $[BF_4]^-$ to $[Tf_2N]^-$ due to decrease of electrostatic interactions in ILs with increasing size of anion from $[BF_4]^-$ to $[Tf_2N]^-$.

2. [Bmim][Y] (Y = BF_4^-, PF_6^-, and Tf_2N^-) ILs Adsorption on the DV-GNF Surface

As shown in Fig S2, $[Bmim]^+$ cation in [Bmim][Y] (Y = BF_4^-, PF_6^-, and Tf_2N^-) ionic liquids tends to take different orientations with respect to the DV-GNF surface. The optimized DV-GNF$[Bmim][BF_4]$ structure is demonstrated in Fig S2. It can be found that the crucial point of $[Bmim][BF_4]$ adsorption is the direct interaction of $[BF_4]^-$ anion with the DV-GNF surface, while interacting closely with the positive part of the $[Bmim]^+$. The triplet fluoride atoms have a distance of 2.904-3.116 Å with the surface of DV-GNF surface. From values of distances, it can be found that the butyl chain is bent slightly downward with respect to the imidazolium ring. In addition, the ring tends parallel to the surface but angles slightly such that the N atom connected to the methyl group is nearer to the surface that the N atom connected to the butyl group. The

alkyl chain of the $[Bmim]^+$ cation is placed almost parallel to the surface such that the distance of the nearest H atoms from the surface is in the range of 2.863-2.954 Å.

In the adsorption of $[Bmim][PF_6]$ IL on the DV-GNF surface, the imidazolium ring tends to be arranged in a parallel orientation with respect to the DV-GNF surface at a distance of 2.870 Å. It can also be found that other carbon atoms of butyl chain are bent slightly upward with respect to imidazolium ring with a weaker interaction relative to the DV-GNF surface in such a way that the distance of the nearest hydrogen atoms is in the range of 2.745-3.833 Å. The three of the fluoride atoms form a plane almost parallel to the imidazolium ring and interact with the surface, although the other three fluoride atoms lie above the imidazolium ring and interact with the H atoms of imidazolium ring, methyl, and butyl groups.

The geometry of DV-GNF$[Bmim][Tf_2N]$ complex is shown in Fig S2. In this structure, one oxygen atom of $-SO_2$ group and two fluoride atoms of $-CF_3$ group in the $[Tf_2N]^-$ anion form a plane parallel to the DV-GNF surface. The $[Tf_2N]^-$ anion tends to interact with the carbon atoms of surface *via* its oxygen and fluoride atoms in the range of 2.908-3.032 Å. The $[Bmim]^+$ cation tends to bend with respect to the DV-GNF surface in such a way that the $[Bmim]^+$ cation interacts with the surface *via* hydrogen atom of C-H bond between two N atoms of imidazolium ring, methyl, and butyl groups. As seen from $[Bmim][Tf_2N]$ structure, the butyl chain of adsorbed $[Bmim]^+$ cation shows a tendency to lie in the plane of the DV-GNF surface. The particular orientation of $[Bmim]^+$ cation in $[Bmim][Tf_2N]$ with respect to the DV-GNF surface seems to be due to the big size of $[Tf_2N]^-$ anion and the competition between cation and anion for interacting with the DV-GNF surface.

3. [Bmim][Y] (Y = BF_4^-, PF_6^-, and Tf_2N^-) ILs Adsorption on the SW-GNF Surface

The geometry structure of ILs on the SW-GNF surface is different from that of ILs on the DV-GNF surface (Fig S2). It seems that the type of defect in the GNF surfaces has an important role in the arrangement and adsorption behavior of ILs on the surfaces. As seen from Fig S2, the geometry structures of $[Bmim][BF_4]$, $[Bmim][PF_6]$, and $[Bmim][Tf_2N]$ ILs are similar on the SW-GNF surface. In these ILs, the imidazolium ring tends to be arranged in a parallel orientation with respect to the SW-GNF surface in such a way that the distance of the nearest hydrogen atoms from the surface is in the range of 2.996-3.479 Å, 2.907-3.751 Å, and 2.888-3.688 Å, respectively. It is worth mentioning that the butyl chain in these structures is bent slightly upward with respect to imidazolium ring with a weaker interaction relative to the SW-GNF

surface in such a way that the distance of the nearest hydrogen atoms from the surface is in the range of 2.472-3.325 Å, 2.629-3.498 Å, and 2.520-3.308 Å, respectively. The three of the fluoride atoms of $[BF_4]^-$ and $[PF_6]^-$ anions and two fluoride atoms from $–CF_3$ group along with one oxygen atom from $–SO_2$ group of $[Tf_2N]^-$ anion form a plane almost parallel to the imidazolium ring and interact with the surface in the range of 2.970-2.994 Å, 2.951-3.107 Å, and 3.013-3.062 Å, respectively. The other fluoride atoms in $[BF_4]^-$ and $[PF_6]^-$ anions and the other fluoride, nitrogen, and oxygen atoms in $[Tf_2N]^-$ anion lie above the imidazolium ring and interact with the H atoms of imidazolium ring, methyl, and butyl groups.

References

[1] M. H. Ghatee and F. Moosavi, *J. Phys. Chem. C*, 2011, **115**, 5626–5636.

[2] M. Shakourian-Fard, G. Kamath, Z. Jamshidi, *J. Phys. Chem. C*, **2014**, *118*, 26003-26016.

[3] M. Shakourian-Fard, Z. Jamshidi, A. Bayat, G. Kamath, *J. Phys. Chem. C* **2015**, *119*, 7095-7108.

Table S1. The results of AIM analysis at the bond critical points (BCPs) between [Bmim][Y] (Y = BF_4^-, PF_6^-, and Tf_2N^-) ILs and DV(SW)-GNF surfaces calculated at the M06-2X/cc-pVDZ level of theory.

Structure	BCP	ρ(r)	∑ρ(r)	$\nabla^2\rho(r)$	G(r)	V(r)	H(r)
IL on the DV-GNF surface							
[Bmim][BF_4]	C29…H81	0.0084	0.0735	0.0287	0.0059	-0.0048	0.0011
	C41…C75	0.0083		0.0252	0.0051	-0.0039	0.0011
	C33…H85	0.0063		0.0208	0.0042	-0.0032	0.0010
	C11…H100	0.0062		0.0201	0.0040	-0.0030	0.0009
	C23…H99	0.0063		0.0188	0.0040	-0.0033	0.0006
	F90…C8	0.0076		0.0316	0.0064	-0.0049	0.0014
	F91…C8	0.0103		0.0430	0.0089	-0.0071	0.0018
	F93…C8	0.0101		0.0426	0.0089	-0.0072	0.0016
	F91…C34	0.0096		0.0401	0.0084	-0.0067	0.0016
[Bmim][PF_6]	C43…H102	0.0060	0.0937	0.0206	0.0040	-0.0029	0.0011
	C20…H102	0.0061		0.0179	0.0038	-0.0031	0.0006
	C6…C75	0.0065		0.0179	0.0038	-0.0031	0.0006
	N73…C7	0.0074		0.0210	0.0046	-0.0040	0.0006
	N71…C41	0.0070		0.0199	0.0044	-0.0038	0.0005
	C29…H90	0.0082		0.0280	0.0055	-0.0041	0.0014
	C14…H93	0.0065		0.0202	0.0041	-0.0032	0.0009
	C14…H94	0.0064		0.0231	0.0045	-0.0034	0.0011
	C2…H94	0.0062		0.0203	0.0043	-0.0035	0.0007
	C50…H94	0.0059		0.0193	0.0041	-0.0033	0.0007
	F84…C51	0.0086		0.0333	0.0070	-0.0058	0.0012
	F87…C52	0.0097		0.0423	0.0088	-0.0070	0.0017
	F83…C16	0.0086		0.0361	0.0075	-0.0059	0.0015
[Bmim][Tf_2N]	C80…H10	0.0055	0.0803	0.0181	0.0036	-0.0028	0.0008
	C46…H6	0.0080		0.0294	0.0058	-0.0043	0.0015
	C47…H6	0.0081		0.0269	0.0057	-0.0048	0.0009
	C74…H14	0.0106		0.0304	0.0068	-0.0060	0.0007
	C75…H20	0.0093		0.0289	0.0062	-0.0053	0.0009
	C89…H24	0.0042		0.0128	0.0025	-0.0019	0.0006
	F37…C83	0.0101		0.0417	0.0090	-0.0075	0.0014
	F36…C82	0.0081		0.0327	0.0069	-0.0057	0.0012
	O29…C61	0.0086		0.0316	0.0067	-0.0055	0.0011
	O29…C47	0.0074		0.0257	0.0054	-0.0045	0.0009
IL on the SW-GNF surface							
[Bmim][BF_4]	C41…H84	0.0075	0.1077	0.0231	0.0050	-0.0043	0.0007
	C27…H84	0.0074		0.0246	0.0052	-0.0043	0.0008
	N73…C13	0.0069		0.0197	0.0044	-0.0038	0.0005
	C12…C76	0.0068		0.0174	0.0037	-0.0031	0.0006
	N75…C36	0.0069		0.0199	0.0043	-0.0036	0.0006

	C35…H89	0.0059		0.0201	0.0041	-0.0031	0.0009
	C7…H90	0.0125		0.0412	0.0091	-0.0079	0.0011
	C16…H98	0.0047		0.0142	0.0029	-0.0023	0.0006
	C22…H85	0.0048		0.0156	0.0030	-0.0022	0.0008
	F92…C45	0.0093		0.0396	0.0082	-0.0064	0.0017
	F95…C32	0.0089		0.0359	0.0075	-0.0060	0.0014
	F94…C31	0.0082		0.0347	0.0071	-0.0056	0.0015
	F94…C45	0.0088		0.0369	0.0076	-0.0061	0.0015
	F94…C22	0.0084		0.0346	0.0071	-0.0056	0.0014
[Bmim][PF_6]	C48…H91	0.0076	0.0756	0.0282	0.0055	-0.0070	0.0015
	C49…C76	0.0049		0.0140	0.0030	-0.0035	0.0004
	C74…C21	0.0085		0.0271	0.0055	-0.0067	0.0012
	N73…C8	0.0053		0.0175	0.0038	-0.0043	0.0005
	C44…H96	0.0098		0.0375	0.0075	-0.0093	0.0018
	F85…C19	0.0082		0.0337	0.0070	-0.0084	0.0014
	F86…C6	0.0072		0.0301	0.0062	-0.0075	0.0013
	F86…C42	0.0072		0.0307	0.0063	-0.0077	0.0013
	F86…C29	0.0072		0.0306	0.0063	-0.0076	0.0013
	F89…C42	0.0093		0.0387	0.0080	-0.0096	0.0016
[Bmim][Tf_2N]	C32..H82	0.0058	0.1018	0.0198	0.0038	-0.0027	0.0011
	C54…H84	0.0060		0.0184	0.0039	-0.0033	0.0006
	C8…H78	0.0063		0.0204	0.0041	-0.0031	0.0009
	C74…C31	0.0082		0.0255	0.0052	-0.0040	0.0011
	C16…C77	0.0058		0.0152	0.0032	-0.0027	0.0005
	C21…H86	0.0113		0.0369	0.0081	-0.0070	0.0011
	C43…H87	0.0086		0.0280	0.0059	-0.0048	0.0010
	C48…H92	0.0031		0.0096	0.0019	-0.0014	0.0004
	C48…H93	0.0030		0.0098	0.0019	-0.0014	0.0005
	F109…C14	0.0072		0.0301	0.0062	-0.0050	0.0012
	F108…C51	0.0074		0.0312	0.0065	-0.0052	0.0012
	F108…C23	0.0075		0.0329	0.0068	-0.0055	0.0013
	O101…C22	0.0066		0.0231	0.0048	-0.0040	0.0009
	O101…C37	0.0065		0.0231	0.0049	-0.0040	0.0008
	O101…C49	0.0079		0.0297	0.0062	-0.0051	0.0011

Table S2. Energy Decomposition Analysis (EDA, in kcal/mol) for DV(SW)-GNF···IL complexes at the PBE-D3/TZP Level of Theory.

Structure	ΔE_{Pauli}	ΔE_{elect}	ΔE_{orb}	ΔE_{disp}	ΔE_{int}[a]
DV-GNF[Bmim][BF_4]	36.96	-17.95(32.2%)	-15.05(27.0%)	-22.76(40.8%)	-18.80
DV-GNF[Bmim][PF_6]	28.11	-14.32(30.1%)	-12.52(26.3%)	-20.67(43.6%)	-19.39
DV-GNF[Bmim][Tf_2N]	31.48	-15.31(29.9%)	-11.53(22.5%)	-24.30(47.6%)	-19.66
SW-GNF[Bmim][BF_4]	35.99	-17.96(31.3%)	-15.25(26.5%)	-24.24(42.2%)	-21.46
SW-GNF[Bmim][PF_6]	33.09	-15.59(29.0%)	-14.25(26.5%)	-23.84(44.5%)	-20.59
SW-GNF[Bmim][Tf_2N]	32.32	-16.63(30.3%)	-11.70(21.3%)	-26.61(48.4%)	-22.61

[a]ΔE_{int} (Interaction energy) values calculated by ADF package are without basis set superposition errors (BSSEs).

Table S3. ChelpG charge analysis calculated at the M06-2X/cc-pVDZ level of theory (charge values are in e).

Structure	q(Cation in IL)	q(Anion in IL)	[a]Δq(Cation)	[b]Δq(Anion)	[c]Δq(Surface)
[Bmim][BF_4]	0.8075	-0.8075			
[Bmim][PF_6]	0.7924	-0.7924			
[Bmim][Tf_2N]	0.7763	-0.7763			
DV-GNF[Bmim][BF_4]	0.7151	-0.6935	0.0924	-0.1140	-0.0216
SW-GNF[Bmim][BF_4]	0.6854	-0.6330	0.1221	-0.1745	-0.0524
DV-GNF[Bmim][PF_6]	0.7340	-0.7629	0.0584	-0.0295	0.0289
SW-GNF[Bmim][PF_6]	0.7556	-0.7541	0.0368	-0.0383	-0.0015
DV-GNF[Bmim][Tf_2N]	0.6802	-0.6624	0.0961	-0.1139	-0.0178
SW-GNF[Bmim][Tf_2N]	0.7878	-0.7830	-0.0115	0.0067	-0.0048
DV-LGNF[Bmim][BF_4]	0.7233	-0.7000	0.0842	-0.1075	-0.0233
SW-LGNF[Bmim][BF_4]	0.6893	-0.6518	0.1182	-0.1557	-0.0375
DV-LGNF[Bmim][PF_6]	0.7430	-0.7579	0.0494	-0.0345	0.0149
SW-LGNF[Bmim][PF_6]	0.7368	-0.715	0.0556	-0.0774	-0.0218
DV-LGNF[Bmim][Tf_2N]	0.7645	-0.7619	0.0118	-0.0144	-0.0026
SW-LGNF[Bmim][Tf_2N]	0.7895	-0.7865	-0.0132	0.0102	-0.0030

[a,b]$\Delta q_{(Cation)}$ and $\Delta q_{(Anion)}$ terms for ILs adsorbed on the DV(SW)-GNF and DV(SW)-LGNF surfaces are as follows: $\Delta q_{(Cation)} = q_{\text{cation in isolated IL (before adsorption)}} - q_{\text{cation in IL (after adsorption)}}$ and $\Delta q_{(Anion)} = q_{\text{anion in isolated IL (before adsorption)}} - q_{\text{anion in IL (after adsorption)}}$. [c]The charge of DV(SW)-GNF and DV(SW)-LGNF surfaces is zero before adsorption of ILs.

Table S4. Calculated excitation energies (E in eV), wavelengths (λ in nm), oscillator strength (f in a.u.) and main configurations computed at the TD-M06-2X/cc-pVDZ level of theory of DV(SW)-GNF surfaces and DV(SW)-GNF[Bmim][Y] (Y = BF_4^-, PF_6^-, and Tf_2N^-) complexes.

Structure	λ(E)	f	Main Transitions	Structure	λ(E)	f	Main Transitions
DV-GNF	649(1.91)	0.0490	HOMO→LUMO	DV-GNF[Bmim][Tf_2N]	720(1.72)	0.0374	HOMO→LUMO
	461(2.69)	0.0150	HOMO-2→LUMO		466(2.66)	0.0071	HOMO-2→LUMO
	385(3.22)	0.1969	HOMO→LUMO+1		390(3.18)	0.2065	HOMO→LUMO+1
	348(3.56)	0.3632	HOMO-1→LUMO+2		357(3.47)	0.2637	HOMO-4→LUMO
SW-GNF	613(2.02)	0.0357	HOMO→LUMO	SW-GNF[Bmim][BF_4]	593(2.09)	0.0418	HOMO→LUMO
	515(2.41)	0.0539	HOMO-1→LUMO		520(2.38)	0.0574	HOMO-1→LUMO
	425(2.92)	0.1226	HOMO-1→LUMO+2		443(2.79)	0.0771	HOMO→LUMO+2
	375(3.30)	0.7488	HOMO→LUMO+1		371(3.34)	0.4936	HOMO-1→LUMO+1
DV-GNF[Bmim][BF_4]	668(1.85)	0.0409	HOMO→LUMO	SW-GNF[Bmim][PF_6]	640(1.93)	0.0277	HOMO→LUMO
	466(2.65)	0.0073	HOMO-2→LUMO		536(2.31)	0.0676	HOMO-1→LUMO
	387(3.20)	0.1606	HOMO→LUMO+1		445(2.78)	0.0641	HOMO→LUMO+2
	357(3.47)	0.3104	HOMO-1→LUMO+2		382(3.24)	0.6539	HOMO→LUMO+1
DV-GNF[Bmim][PF_6]	668(1.85)	0.0460	HOMO→LUMO	SW-GNF[Bmim][Tf_2N]	617(2.01)	0.0344	HOMO→LUMO
	471(2.63)	0.0049	HOMO-2→LUMO		525(2.36)	0.0613	HOMO-1→LUMO
	385(3.21)	0.2110	HOMO→LUMO+1		442(2.80)	0.0752	HOMO→LUMO+2
	349(3.54)	0.2609	HOMO-1→LUMO+2		376(3.29)	0.5031	HOMO-1→LUMO+2

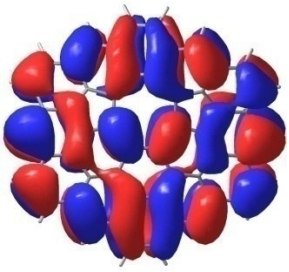

DV-GNF-HOMO

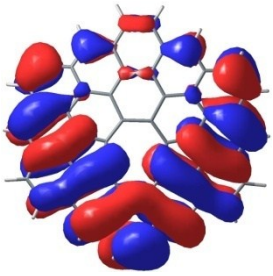

DV-GNF-HOMO-1

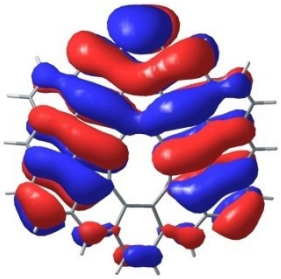

DV-GNF-HOMO-2

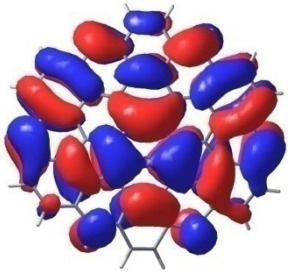

DV-GNF-LUMO

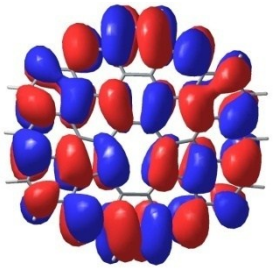

DV-GNF-LUMO+1

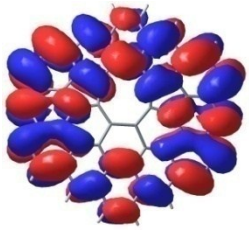

DV-GNF-LUMO+2

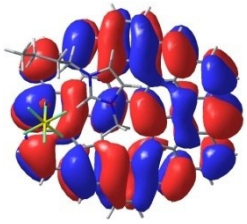

DV-GNF[Bmim][PF_6]-HOMO

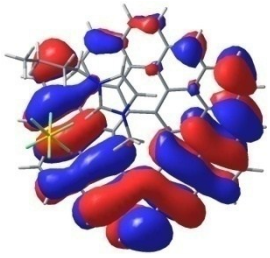

DV-GNF[Bmim][PF_6]-HOMO-1

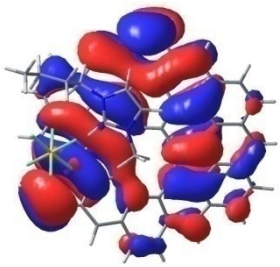

DV-GNF[Bmim][PF_6]-HOMO-2

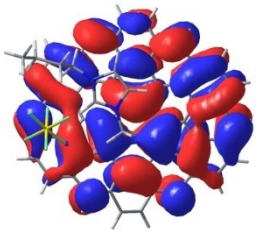

DV-GNF[Bmim][PF_6]-LUMO

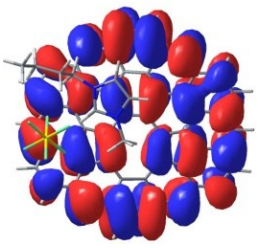

DV-GNF[Bmim][PF_6]-LUMO+1

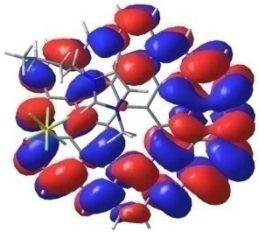

DV-GNF[Bmim][PF_6]-LUMO+2

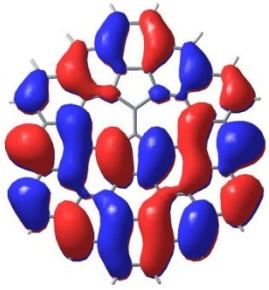

SW-GNF-HOMO

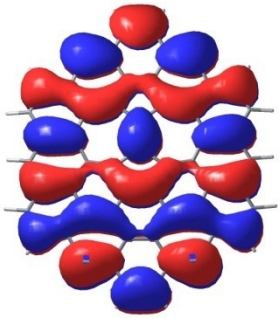

SW-GNF-HOMO-1

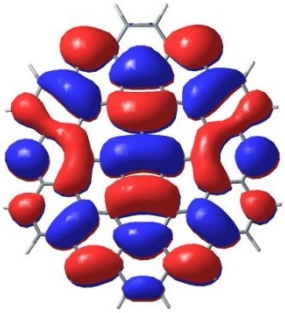

SW-GNF-LUMO

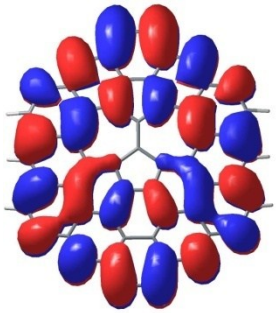

SW-GNF-LUMO+1

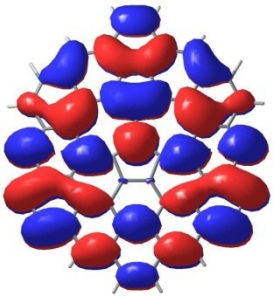

SW-GNF-LUMO+2

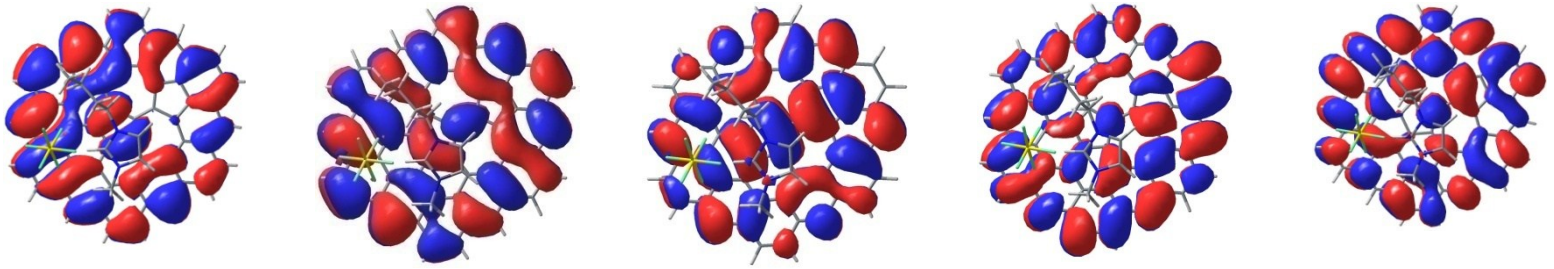

SW-GNF[Bmim][PF_6]-HOMO | SW-GNF[Bmim][PF_6]-HOMO-1 | SW-GNF[Bmim][PF_6]-LUMO | SW-GNF[Bmim][PF_6]-LUMO+1 | SW-GNF[Bmim][PF_6]-LUMO+2

Fig S3. The iso-surfaces of molecular orbitals of DV(SW)-GNF surfaces and DV(SW)-GNF[Bmim][PF_6] complexes calculated at the M06-2X/cc-pVDZ level of theory.

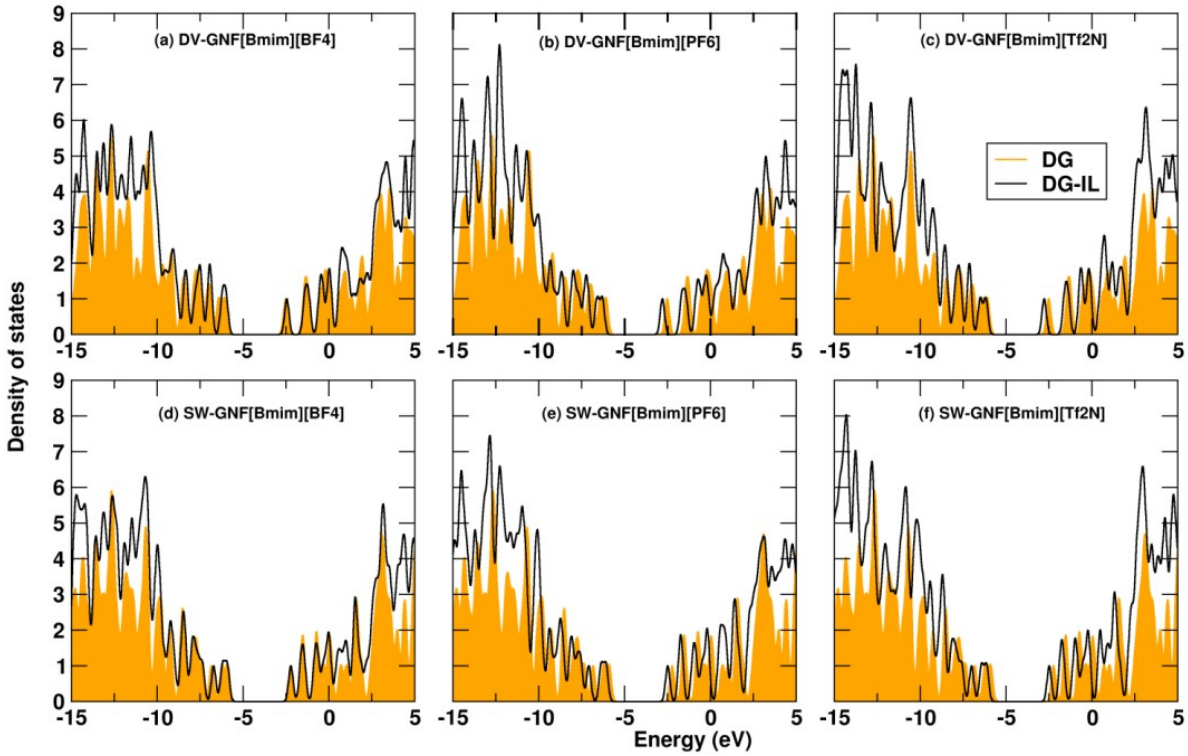

Fig S4. The density of states (DOS) of DV(SW)-GNF surfaces and their complexes with [Bmim][Y] (Y = BF_4^-, PF_6^-, and Tf_2N^-) ILs calculated at the M06-2X/cc-pVDZ level of theory.

Table S5. Energies of HOMO (ε_{HOMO}) and LUMO (ε_{LUMO}) levels, HOMO-LUMO energy gaps (E_g), chemical potential (μ), chemical hardness (η), global softness (S) and electrophilicity index (ω) for the nanoflakes and their complexes with ILs (All energy values are in eV units).

Structure	ε_{HOMO}	ε_{LUMO}	^aE_g	μ	η	$S = 1/\eta$	ω
SW-GNF	-5.90	-2.22	3.68	-4.06	1.84	0.543	4.479
DV-GNF	-6.08	-2.51	3.57	-4.29	1.78	0.560	5.167
DV-GNF[Bmim][BF_4]	-5.99	-2.45	3.54	-4.22	1.77	0.565	5.031
DV-GNF[Bmim][PF_6]	-6.29	-2.79	3.5	-4.54	1.75	0.571	5.889
DV-GNF[Bmim][Tf_2N]	-6.18	-2.77	3.41	-4.47	1.70	0.586	5.872
SW-GNF[Bmim][BF_4]	-5.92	-2.21	3.71	-4.06	1.85	0.539	4.454
SW-GNF[Bmim][PF_6]	-6.08	-2.48	3.60	-4.28	1.80	0.555	5.088
SW-GNF[Bmim][Tf_2N]	-6.13	-2.48	3.65	-4.30	1.82	0.548	5.077
SW-LGNF	-5.49	-2.50	2.99	-3.99	1.49	0.668	5.337
DV-LGNF	-5.67	-3.04	2.63	-4.35	1.31	0.760	7.211
DV-LGNF[Bmim][BF_4]	-5.59	-2.85	2.74	-4.22	1.37	0.729	6.499
DV-LGNF[Bmim][PF_6]	-5.69	-3.16	2.53	-4.42	1.26	0.790	7.739
DV-LGNF[Bmim][Tf_2N]	-5.72	-3.08	2.64	-4.40	1.32	0.757	7.333
SW-LGNF[Bmim][BF_4]	-5.43	-2.50	2.93	-3.96	1.46	0.682	5.365
SW-LGNF[Bmim][PF_6]	-5.60	-2.63	2.97	-4.11	1.48	0.673	5.701
SW-LGNF[Bmim][Tf_2N]	-5.75	-2.79	2.96	-4.27	1.48	0.675	6.159
GNF	-6.09	-1.77	4.32	-3.93	2.16	0.463	3.575
GNF[Bmim][BF_4]	-6.13	-1.90	4.23	-4.01	2.11	0.473	3.811
GNF[Bmim][PF_6]	-6.22	-1.98	4.24	-4.10	2.12	0.472	3.965
GNF[Bmim][Tf_2N]	-6.22	-1.94	4.28	-4.08	2.14	0.467	3.889
h-BNNF	-8.10	0.88	8.98	-3.61	4.49	0.223	1.451
h-BNNF[Bmim][BF_4]	-7.89	0.03	7.92	-3.93	3.96	0.252	1.950
h-BNNF[Bmim][PF_6]	-7.83	0.28	8.11	-3.77	4.05	0.247	1.757
h-BNNF[Bmim][Tf_2N]	-7.62	0.06	7.68	-3.78	3.84	0.260	1.860

$^aE_g = \varepsilon_{(LUMO)} - \varepsilon_{(HOMO)}$